ISSN: 2977-4047

Journal of Life Sciences Research and Reviews

SCIENTIFIC Research and Community

Research Article

Open Access

The Mechanism of Graft Compatibility: Mineral Element Synergy in a Pluot-Apricot System

Miansen Lei[1,2], Yongqiang Huang[1,2], Tianfa Guo[1,2], Ming Wang[3] and Xinjian Wang[1,2]*

[1]College of Horticulture and Forestry, Tarim University, Alar, Xinjiang, PR China

[2]National-Local Joint Engineering Laboratory of High Efficiency and Superior Quality Cultivation and Fruit Deep Processing Technology on Characteristic Fruit Trees, Alar, Xinjiang, PR China

[3]Xinjiang Academy of Forestry, Urumqi, Xinjiang, PR China

ABSTRACT

'Dinosaur Egg' (*Prunus domestica × P. armeniaca* Konglongdan) pluot grafted onto Siberian apricot (*Armeniaca sibirica* (L.) Lam.) rootstocks exhibited incompatibility symptoms five years post-grafting, including leaf yellowing, abnormal swelling at the graft union, growth retardation, and weakened tree vigor. These symptoms led to plant breakage under high winds, causing significant economic losses in agricultural production. However, research on graft compatibility in 'Dinosaur Egg' remains limited. This study therefore investigates mineral element dynamics by quantifying twelve elements - nitrogen (N), phosphorus (P), potassium (K), calcium (Ca), magnesium (Mg), iron (Fe), manganese (Mn), copper (Cu), zinc (Zn), boron (B), molybdenum (Mo), and sodium (Na) - in rootstocks and scions of compatible and incompatible graft combinations. Through significance analysis, correlation analysis, and principal component analysis, this study investigates the relationship between the mineral element content of rootstock–scion and the graft compatibility in 'Dinosaur Egg' pluot. Results demonstrated that in compatible 'Dinosaur Egg' graft combinations, concentrations of metal cations (K, Ca, Mg) and trace elements (Cu, Zn) were significantly higher than in incompatible combinations. Elements exhibited predominantly positive correlations, with only Cu and Mo forming an antagonistic pair, collectively establishing a stable "Cu-core + multi-element synergy" network. Conversely, incompatible combinations showed abnormal elevations in N, P, Fe, Mo, and Na concentrations, with disordered elemental associations forming a discordant "Mo-Na localized synergy + Na-K antagonistic pair" pattern. Principal component analysis revealed clear separation between compatible and incompatible combinations along PC1 and PC2 dimensions. Reduced compatibility likely contributes to excessive N and P accumulation in scions and impaired transport of K, Fe, and Cu.

***Corresponding author**

Xinjian Wang, College of Horticulture and Forestry, Tarim University, Alar, Xinjiang, PR China; National-Local Joint Engineering Laboratory of High Efficiency and Superior Quality Cultivation and Fruit Deep Processing Technology on Characteristic Fruit Trees, Alar, Xinjiang, PR China.

Received: January 17, 2026; **Accepted:** January 21, 2026; **Published:** January 30, 2026

Keywords: Correlation Analysis, Graft Union, Ionic Homeostasis, Nutrient Transport, Principal Component Analysis, Vegetative Growth

Introduction

The 'Dinosaur Egg'(Prunus domestica × P. armeniaca 'Konglongdan') pluot is a fruit tree belonging to the genus Prunus in the Rosaceae family [1]. It is a new interspecific hybrid fruit that was selected in the 1990s after more than 70 years of research by several generations of American breeding specialists, who crossed apricot (Prunus armeniaca L.) and plum (Prunus domestica L.) [2]. In 2001, the Research Institute of Non - timber Forestry, Chinese Academy of Forestry screened out the variety following the introduction of the national "948" project. Of these, the genes of the plum varieties account for approximately 75%, and the genes of the apricot varieties account for approximately 25% [3,4]. The 'Dinosaur Egg' pluot possesses significant nutritional value and is highly favored by consumers [4,5]. It has been acclaimed as the "fruit prodigy of the 21st century" and demonstrates considerable economic potential [6]. As of 2023, the cultivation area of pluot in China continues to expand, with Xinjiang Uygur Autonomous Region region alone reaching a planting area of 6,670 hectares [7].

Grafting, as an ancient yet pivotal technique in plant propagation and improvement, offers significant advantages such as preserving superior maternal traits, enhancing plant stress resistance, and promoting early and abundant yields [8,9]. The rapid expansion of pluot cultivation areas is inextricably linked to the widespread application of grafting technology. Research has demonstrated that grafting success is largely determined by graft compatibility [10]. Highly compatible graft combinations ensure high survival rates of grafted seedlings, vigorous growth, and high-quality fruit production. In contrast, poor compatibility may result in graft failure, growth inhibition, or reduced fruit quality [11]. Structural disorders arising from graft incompatibility led to compromised mechanical strength at the graft union, which may predispose the union to fracture under strong winds or after several years, thereby resulting in substantial economic losses [12]. To date, issues related to graft incompatibility remain a persistent challenge in many agricultural production systems [13,14].

Research has demonstrated that grafting significantly influences the efficiency of mineral element absorption, translocation, and utilization in plants [15]. Mineral elements are essential for plant growth, enhancing plant vigor both indirectly-by modulating oxidoreductase activity or altering root exudates-and directly through regulating microbial community dynamics, soil nutrient content and pH fluctuations in the rhizosphere, as well as lignin deposition and phytoalexin biosynthesis [16]. Plants exhibit specific deficiency symptoms when a particular mineral element is lacking [17]. Moreover, requirements for the same element may vary across plant species, and deficiency symptoms often differ among elements [18,19]. Furthermore, mineral element demand fluctuates throughout various developmental stages [20]. However, deficiency symptoms for a given element are generally consistent across species, and deficiencies in any element tend to suppress plant growth and tree vigor to some extent [21,22].

Research on rootstocks for pluot remains limited to date. Current studies have primarily focused on a narrow range of materials, including Nanking cherry (Prunus tomentosa), peach (Prunus persica), and Chinese plum (Prunus salicina), Siberian apricot (Armeniaca sibirica (L.) Lam.) and David peach (Prunus davidiana), However, these investigations are generally characterized by insufficient methodological depth and lack systematic evaluation [23-26]. Field investigations indicate that the primary rootstocks used for pluot in Xinjiang are David peach and Siberian apricot. Graft incompatibility has been observed in 'Dinosaur Egg' scions grafted onto Siberian apricot rootstocks, typically beginning five years after grafting. These symptoms have resulted in 11.9% incidence of foliar chlorosis and 1.7% mortality due to wind-induced breakage at the graft junction, leading to substantial economic losses in local agricultural production. In grafting systems, rootstocks-typically seedling-grown plants-serve as critical regulators of plant responses to diverse abiotic and biotic stressors, including pathogens, water/nutrient deficiencies, and potentially toxic compounds (e.g., salts or heavy metals)-rootstocks exhibit significant structural and functional variability among different varieties [27-29]. In this study, graft-compatible and incompatible combinations were used as reciprocal controls to investigate the relationship between graft compatibility of 'Dinosaur Egg' plum on Siberian apricot rootstocks and the contents of 12 mineral elements in both rootstocks and scions. We analyzed differences in mineral element profiles between compatible and incompatible graft unions, with the goal of elucidating the synergistic effects of mineral elements and their correlation with graft compatibility. These findings are expected to provide a scientific basis for rootstock breeding and rational fertilization strategies in pluot cultivation.

Materials and Methods

Plant Materials and Treatments

The experimental site is situated in Wensu County, Aksu Region, Xinjiang Uygur Autonomous Region, China (80°11′37″N, 41°24′36″E; elevation: 1301 m), featuring a typical warm-temperate continental arid climate. The region experiences an average annual sunshine duration of 2800-3000 hours, mean annual precipitation of 42.4 to 94 mm, mean annual evaporation of 1948 mm, mean annual temperature of 10.1 °C, extreme minimum temperature of -27.6 °C, and a frost-free period of 180-227 days. Situated on an alluvial fan plain at the southern foothills of the Tianshan Mountains, the terrain is flat and open. The soil is classified as Brown Desert Soil with the following characteristics: pH 7.33; organic matter 0.39%; available phosphorus 12.87 $mg \cdot kg^{-1}$, available potassium 184.82 $mg \cdot kg^{-1}$, alkali-hydrolyzable nitrogen 13.68 $mg \cdot kg^{-1}$.

This study employed eight-year-old 'Dinosaur Egg' pluot trees grafted onto Siberian apricot rootstocks as experimental materials. Trees were planted at a spacing of 3 m × 5 m. All field management practices-including irrigation, fertilization, and pest control-followed standard commercial orchard protocols.

Sampling was performed on April 11, 2025. Scion samples of both compatible and incompatible 'Dinosaur Egg' combinations were collected by selecting branches of similar age and diameter from six individual grafted plants (n = 6) showing compatibility or incompatibility traits, with samples taken from each of the four cardinal directions (east, south, west, and north). Rootstock samples were obtained from root suckers of Siberian apricot located at the base of the same six grafted plants (n = 6), again selecting basal shoots of comparable age and diameter. Samples consisting of approximately 5 cm long rootstock and scion branch segments were prepared by pooling 24 branch segments per treatment to form one composite sample, with three biological replicates per group. Following collection, all samples were immediately placed in insulated containers for low-temperature preservation. Subsequent processing included rinsing with tap water, washing with distilled water, enzyme inactivation at 105 °C, drying at 70 °C, grinding, and sieving through a 0.55 mm mesh. The final powdered samples were stored in desiccators for further analysis.

Main Morphological Character in Graft Combinations with Differential Compatibility

Based on methodologies established in apricot, plum, and peach grafting studies by, symptoms of "translocated" graft-incompatibility in the 'Dinosaur Egg' were assessed through visual diagnosis of leaf characteristics, tree vigor, and graft union morphology [30-33]. On August 11, 2024, key morphological traits were measured using eight-year-old grafted plants with either compatible or incompatible unions. Parameters included plant height, crown diameter, shoot growth increment, shoot diameter, graft union diameter, and stem diameters at 5 cm above and below the graft junction. The relative chlorophyll content per unit leaf area was estimated under field conditions using a SPAD-502 Plus chlorophyll meter (Beijing Harvesting Science And Technology Co., Ltd., China) [34]. For each graft compatibility combination, six trees were selected, and 30 mature leaves from the outer canopy were randomly sampled for SPAD measurement.

Determination of Mineral Element Content in Plant Tissues

Mineral element quantification was performed from April 22 to 30, 2025. Pre-treatment of scion and rootstock materials from compatible/incompatible 'Dinosaur Egg' grafts followed the protocols described by and Lou et al. (2008) [35]. Total nitrogen (N) and phosphorus (P) contents were determined using a continuous flow analyzer (Chem450, AMS, Italy), while total potassium (K), calcium (Ca), magnesium (Mg), iron (Fe), manganese (Mn), copper (Cu), zinc (Zn), boron (B), molybdenum (Mo), and sodium (Na) were quantified by inductively coupled plasma mass spectrometry (NexION 1000G ICP-MS, PerkinElmer, USA) [36,37]. Three biological replicates were analyzed per sample group.

Statistical Analysis

Statistical analyses were conducted using IBM SPSS Statistics 27 (United States) and Origin 2024 (United States). Data from three biological replicates per graft component (scion and rootstock) of both compatible and incompatible 'Dinosaur Egg' combinations were compiled and analyzed. Mean values and standard deviations were computed as indicators of mineral content for each compatibility group. One-way analysis of variance (ANOVA) was performed in SPSS to compare group means. When ANOVA yielded significant F-values ($P \leq 0.05$), Duncan's multiple range test was applied for post-hoc mean separation. Pearson correlation analyses were performed to assess the relationships among mineral elements across compatibility groups using SPSS, with the significance level set at $p \leq 0.05$. Two-dimensional correlation heatmaps based on mean values of biological replicates were generated with Origin 2024. Principal component analysis (PCA) of the twelve mineral elements was carried out in SPSS, and biplots illustrating the integrated scion-rootstock systems were visualized using Origin 2024.

Results

Graft Compatibility MO Influence Vegetative Growth in 'Dinosaur Egg'

Visual diagnosis and principal tree architecture traits of 'Dinosaur Egg' pluot grafted onto Siberian apricot rootstocks revealed that compatible combinations exhibited normal tree height with healthy shoots and leaves (Table 1 and Figure 1A). Crown diameter, current-year shoot length, stem diameter (of current-year shoot), and relative chlorophyll content all significantly exceeded those of incompatible combinations (Table 1). Furthermore, the graft unions were well-healed without visible swelling (Figure 1C), and no significant differences were detected in diameters at 5 cm above the graft union, 5 cm below the graft union, and at the graft union (Table 1). In contrast, graft-incompatible 'Dinosaur Egg' combinations exhibited typical symptoms of the "translocated" incompatibility. The overall tree height was approximately 20% lower than that of compatible grafts (Table 1). Leaves showed mild curling and yellowing/reddening (Figure 1B), while crown diameter, current-year shoot length, stem diameter (of current-year shoot), and relative chlorophyll content were all significantly reduced (Table 1). In particular, the current-year shoot length was only 36%, and relative chlorophyll content was less than half of that in compatible plants (Table 1). Furthermore, pronounced swelling and cracking were observed at the graft union (Figure 1D), where the diameter was significantly larger than at positions 5 cm above and below the union (Table 1).

Table 1: Main Tree Growth Characteristics of Compatible and Incompatible 'Dinosaur Egg' Graft Unions

Morphological Parameters Measured	Compatible Grafts	Incompatible Grafts
Tree height (m)	4.16 ± 0.29	3.39 ± 0.50
East-west crown diameter (m)	5.02 ± 0.77	3.27 ± 0.59
North-south crown diameter (m)	4.39 ± 0.65	2.74 ± 0.39
Current-year shoot length (cm)	58.91 ± 4.83	21.23 ± 5.25
Stem diameter (of current-year shoot) (mm)	8.21 ± 0.90	4.06 ± 0.48
Chlorophyll (a+b) content	36.14 ± 3.24	11.60 ± 1.85
Diameter at 5 cm below graft union (cm)	12.89 ± 2.61 a	12.89 ± 1.72 b
Graft union diameter (cm)	13.59 ± 2.21 a	16.18 ± 1.16 a
Diameter at 5 cm above graft union (cm)	11.88 ± 3.27 a	13.16 ± 2.93 b

X ± S = Mean ± Standard Deviation of compatible and incompatible graft combinations of 'Dinosaur Egg' (n = 3 biological replicates). According to Duncan's Multiple Range Test, diameters at 5 cm above the graft union, 5 cm below the graft union, and at the graft union itself were analyzed separately separately for compatible and incompatible 'Dinosaur Egg' grafts.. Within each column, mean values followed by different lowercase letters (a, b) indicate significant differences at the $P \leq 0.05$ level.

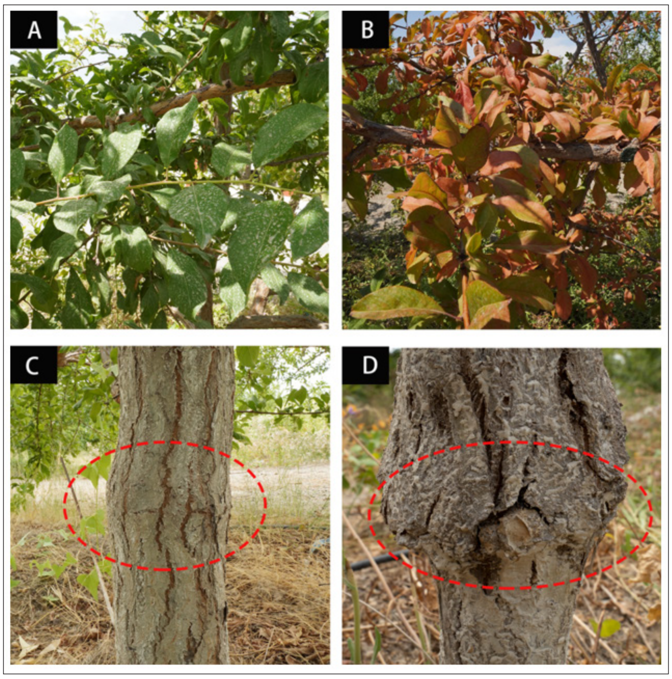

Figure 1: Visual Diagnosis of Selective Graft Incompatibility in 'Dinosaur Egg' Pluot Grafted onto Siberian Apricot Rootstock Eight Years After Grafting: Healthy Shoot and Foliage in a Compatible Combination (A); External Symptoms of Translocated Incompatibility, including Leaf Curling and Yellowing/Reddening (B); Well-Healed Graft union without significant Swelling in a Compatible Combination (C); Swelling and Cracking at the Graft Union Site in an Incompatible Combination (D).

Comparative Analysis of Mineral Elements in 'Dinosaur Egg' pluot Branch Tissues with Differential Graft Compatibility

Long-term graft compatibility analysis of 'Dinosaur Egg' on Siberian Apricot rootstocks revealed differential mineral element accumulation between compatible and incompatible grafts (Table 2). Among twelve elements analyzed (N, P, K, Ca, Mg, Fe, Mn, Cu, Zn, B, Mo, Na), compatible grafts exhibited moderately higher contents of K, Ca, Mg, Mn, Cu, Zn, and B. In contrast, incompatible grafts showed marginally elevated levels of N, P, Fe, Mo, and Na compared to compatible combinations.

Table 2: Mineral Element Contents in 'Dinosaur Egg' Branches from Compatible and Incompatible Grafts(mg·kg^{-1})

Mineral Element	Compatible Grafts	Incompatible Grafts
N	7367.35 ± 795.79	9030.65 ± 843.11
P	1165.22 ± 47.99	1251.07 ± 64.77
K	4642.94 ± 216.38	4490.74 ± 239.28
Ca	3041.46 ± 112.59	2462.26 ± 217.30
Mg	1339.53 ± 122.16	1203.87 ± 33.26
Fe	51.49 ± 5.69	55.61 ± 5.76
Mn	23.25 ± 1.57	17.24 ± 0.99
Cu	4.35 ± 0.51	3.08 ± 0.31
Zn	11.59 ± 0.81	8.99 ± 0.62
B	26.30 ± 0.83	23.88 ± 1.23
Mo	0.67 ± 0.07	0.78 ± 0.05
Na	437.00 ± 20.74	483.16 ± 38.77

X ± S = Mean ± Standard Deviation of compatible/incompatible graft combinations (n = 3 biological replicates).

Comparative analysis of mineral elements in scions and rootstocks revealed significant differences in their distribution between compatible and incompatible graft combinations of 'Dinosaur Egg' (Table 3). In scions, no significant differences were detected in Fe, Mo, or Na content between compatibility types. However, incompatible scions contained significantly higher N (40.02%), P (33.45%), and K (7.21%) compared to compatible scions. In contrast, compatible scions exhibited significantly greater concentrations of Ca (29.46%), Mg (15.22%), Mn (31.09%), Cu (20.27%), Zn (17.49%), and B (21.67%) than incompatible scions. In rootstocks, no significant differences were observed in N, Ca, Mg, Fe, Mn, B, or Mo content between compatibility groups. Compatible rootstocks showed significantly higher content of P (33.29%), K (16.52%), Cu (70.85%), and Zn (56.43%) than incompatible rootstocks. Conversely, Na content was significantly higher (53.00%) in incompatible rootstocks compared to compatible ones.

Table 3: Mineral Element Contents in Rootstock–Scion Systems of Compatible and Incompatible 'Dinosaur Egg' Graftsafts(mg·kg^{-1})

Mineral Element	Compatible Grafts		Incompatible Grafts	
	Scion	Rootstock	Scion	Rootstock
N	8344.06 ± 368.46 b	6413.06 ± 1216.09 c	11683.02 ± 2199.70 a	6290.29 ± 665.84 c
P	1286.67 ± 84.18 b	1043.64 ± 112.67 c	1717.09 ± 218.54 a	782.96 ± 75.62 d
K	4765.87 ± 379.58 b	4508.12 ± 398.35 b	5109.70 ± 156.12 a	3868.94 ± 414.50 c
Ca	3852.59 ± 315.53 a	2215.24 ± 425.78 c	2975.78 ± 573.35 b	1947.33 ± 203.21 c
Mg	1506.25 ± 222.46 a	1171.72 ± 199.48 bc	1307.25 ± 129.81 b	1100.32 ± 88.22 c
Fe	55.17 ± 10.08 ab	46.90 ± 8.95 b	62.93 ± 7.64 a	48.27 ± 8.44 b
Mn	27.32 ± 4.87 a	17.06 ± 2.99 c	20.84 ± 3.77 b	13.63 ± 2.63 c
Cu	4.45 ± 0.55 a	4.22 ± 0.47 a	3.70 ± 0.56 b	2.47 ± 0.13 c
Zn	14.71 ± 0.70 a	8.51± 0.79 c	12.52 ± 1.25 b	5.44 ± 0.19 d
B	31.39 ± 3.87 a	21.66 ± 3.67 c	25.80 ± 2.16 b	21.95 ± 3.19 c
Mo	0.67 ± 0.13 a	0.68 ± 0.08 a	0.73 ± 0.12 a	0.77 ± 0.14 a
Na	541.04 ± 99.97 a	326.23 ± 130.20 b	467.31 ± 45.11 a	499.12 ± 96.56 a

X ± S = Mean ± Standard Deviation of scion/rootstock components under compatible/incompatible grafts (n = 3 biological replicates). Mean values within the same row followed by different letters (a,b,c,d) are significantly different at P ≤ 0.05 according to Duncan's Multiple Range Test.

Analysis of mineral element distribution in rootstock–scion combinations of compatible and incompatible 'Dinosaur Egg' grafts (Table 3) revealed significantly higher concentrations of N, P, Ca, Mg, Mn, Zn, and B in scions compared to their corresponding rootstocks in both compatibility types. Specifically, in compatible combinations, scions exhibited 30.11% higher N, 23.29% higher P, and 72.86% higher Zn than rootstocks. In incompatible combinations, scion concentrations of N, P, and Zn were approximately double those in rootstocks. No significant differences were observed between scions and rootstocks in K, Fe, Cu, or Mo content in compatible combinations. However, in incompatible combinations, only Mo showed no significant difference between scions and rootstocks. Scions in incompatible combinations demonstrated 32.07% higher K, 30.37% higher Fe, and 49.80% higher Cu content compared to their rootstocks. Additionally, while Na levels showed no significant difference between scions and rootstocks in incompatible combinations, compatible scions contained 65.85% higher Na than compatible rootstocks.

Correlation Analysis of Mineral Elements in 'Dinosaur Egg' pluot Branches with Differing Grafting Affinities

Correlation Analysis of Mineral Elements in Grafted Compatible 'Dinosaur Egg' pluot Combinations

The analysis of correlations among 12 mineral elements in graft-compatible 'Dinosaur Egg' combinations revealed significant inter-element relationships (Figure 2A). N showed highly significant positive correlations ($p < 0.01$) with seven elements including P, Ca, and Mn. Phosphorus exhibited highly significant positive correlations ($p < 0.01$) with five elements including Ca and Mn. K demonstrated highly significant positive correlations ($p < 0.01$) with Fe, Mn, and B. Both Ca and Mg showed highly significant positive correlations ($p < 0.01$) with multiple elements. Fe, Mn, Zn, and B exhibited highly significant positive correlations ($p < 0.01$) with various other elements in multiple combinations. B also demonstrated a highly significant positive correlation ($p < 0.01$) with Na, while Cu showed an exclusively negative correlation with Mo ($p < 0.01$) that was distinct from the predominant positive correlation network. Overall, mineral elements in compatible 'Dinosaur Egg' grafts displayed extensive positive correlations, with the Cu-Mo pair constituting the sole antagonistic relationship.

Correlation analysis of 12 mineral elements in scion-grafted 'Dinosaur Egg' combinations revealed a complex network of positive and negative inter-element relationships (Figure 2B). In the scions, N exhibited a highly significant negative correlation ($p < 0.01$) with K, Fe, Mn, and Cu, while demonstrating a highly significant positive correlation ($p < 0.01$) with Mo. P exhibited a highly significant negative correlation ($p < 0.01$) exclusively with Ca. K exhibited a highly significant negative correlation ($p < 0.01$) with Mo, and a highly significant positive correlation ($p < 0.01$) with Fe, Mn, and Cu. Fe exhibited a highly significant negative correlation ($p < 0.01$) with Mo, and a highly significant positive correlation ($p < 0.01$) with Mn, Cu, B, and Na. Both Cu and B exhibited highly significant negative correlations ($p < 0.01$) with Mo, while Mo also exhibited a highly significant negative correlation ($p < 0.01$) with Na. Ca exhibited a highly significant positive correlation ($p < 0.01$) solely with Zn. Mg exhibited highly significant positive correlations ($p < 0.01$) with B and Na. Mn exhibited a highly significant negative correlation ($p < 0.01$) with Mo, and highly significant positive correlations ($p < 0.01$) with Cu and B. Overall, Mo functioned as an antagonistic hub, forming a distinct negative correlation centre independent of the primary network, while metal cations (K, Ca, Mg, Fe, Mn, Cu, Zn) formed interconnected clusters through positive interconnections.

Correlation analysis of 12 mineral elements in rootstocks of graft-compatible 'Dinosaur Egg' combinations revealed (Figure 2C) that N, P, Ca, Fe, Mn, Zn, and Na all exhibited highly significant negative correlations ($p < 0.01$) with Cu. B and Mo showed significant negative correlations ($p < 0.05$) with Cu, forming an independent Cu antagonistic centre within the network. N and P each exhibited highly significant positive correlations ($p < 0.01$) with Ca, Fe, Mn, Zn, B, Mo, and Na, forming a tightly interconnected synergistic network. Pairwise combinations among Ca, Fe, and Mn each showed highly significant positive correlations ($p < 0.01$) with Zn, B, Mo, and Na. Furthermore, Fe and Mn exhibited highly significant positive correlations ($p < 0.01$) with each other, as did Zn, B, and Mo among themselves, collectively constituting the main synergistic network. Overall, the elements formed a complex network characterized by multi-element synergistic positive correlations cantered on N and P as the core, coordinated with elements such as Ca and Fe, while Cu functioned as the antagonistic centre.

Correlation analysis of mineral elements between scions and rootstocks in compatible 'Dinosaur Egg' graft combinations revealed (Figure 2D) that N in scions exhibited a highly significant negative correlation ($p < 0.01$) with Cu in rootstocks, but highly significant positive correlations ($p < 0.01$) with N, P, Ca, Fe, Mn, Zn, B, Mo, and Na in rootstocks. P in scions exhibited a highly significant negative correlation ($p < 0.01$) exclusively with Mg in rootstocks. K in scions exhibited highly significant negative correlations ($p < 0.01$) with N, P, Ca, Fe, Mn, Zn, B, Mo, and Na in rootstocks, while exhibiting a highly significant positive correlation ($p < 0.01$) with Cu in rootstocks. Ca in scions exhibited a highly significant negative correlation ($p < 0.01$) with Cu in rootstocks and a highly significant positive correlation ($p < 0.01$) with Mg in rootstocks. Mg in scions exhibited a highly significant negative correlation ($p < 0.01$) with K in rootstocks and a highly significant positive correlation ($p < 0.01$) with Mg in rootstocks. Fe, Mn, and Cu in scions all exhibited highly significant negative correlations ($p < 0.01$) with N, P, Ca, Fe, Mn, Zn, B, and Mo in rootstocks, and positive correlations with Cu in rootstocks ($p < 0.05$). Both Zn and Mo in scions exhibited negative correlations with Cu in rootstocks; specifically, Mo in scions exhibited highly significant positive correlations ($p < 0.01$) with N, P, Ca, Fe, Mn, Zn, B, and Mo in rootstocks, while Zn in scions exhibited highly significant positive correlations ($p < 0.01$) with N, P, Ca, Fe, Mn, and Zn in rootstocks. Both B and Na in scions exhibited highly significant negative correlations ($p < 0.01$) with K, B, and Mo in rootstocks. The overall analysis reveals a network characteristic in which Cu in the rootstock serves as a negative regulatory hub, while complex synergistic and antagonistic relationships exist between elements such as N and K in the scion and multiple elements in the rootstock.

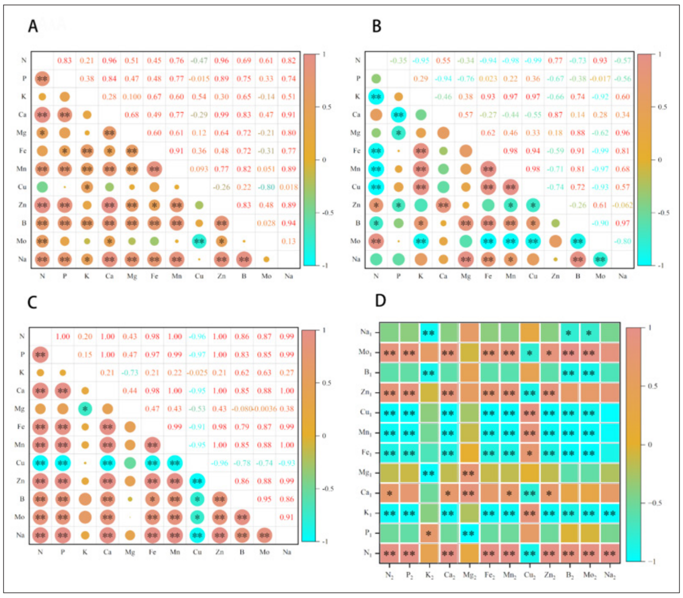

Figure 2: Pearson's Correlation Coefficients of Mineral Elements in the Graft-Compatible 'Dinosaur Egg' Pluot Combination: Correlation Matrix of 12 Mineral Elements in Graft-Compatible 'Dinosaur Egg' Combinations (A); Correlation Matrix of 12 Mineral Elements in Scions of Graft-Compatible 'Dinosaur Egg' Combinations (B); Correlation Matrix of 12 Mineral Elements in Rootstocks of Graft-Compatible 'Dinosaur Egg' combinations (C); Correlation Matrix of Mineral Elements between Scions and Rootstocks in Graft-Compatible 'Dinosaur Egg' Combinations (D). In (A, B, C, D), Red indicates Positive Correlations and Blue Indicates Negative Correlations, * Represented the Significant Difference at $P < 0.05$ level, and ** Represented the Significant Difference at $P < 0.01$ level. (D)The Subscript "1" on the Ordinate (Y-axis) Denotes the scion, while the Subscript "2" on the Abscissa (X-axis) Represents the Rootstock.

Correlation Analysis of Mineral Elements in Grafted Incompatibility 'Dinosaur Egg' pluot Combinations Correlation analysis of 12 mineral elements in graft-incompatible 'Dinosaur Egg' assemblages (Figure 3A) revealed that N was highly significantly positively correlated with P, K, Mg, Cu, Zn, and B ($p < 0.01$). P exhibited highly significant positive correlations with K, Fe, Cu, and Zn ($p < 0.01$). K showed highly significant negative correlation with Na ($p < 0.01$) but highly significant positive correlations with Zn and B ($p < 0.01$). Furthermore, Ca displayed strong positive correlations with Mg and Mn ($p < 0.01$); Mg with Mn and Zn ($p < 0.01$); Fe with Cu and Zn ($p < 0.01$); Cu with Zn and B ($p < 0.01$); Zn with B ($p < 0.01$); and Mo with Na ($p < 0.01$). The overall structure exhibits a positive correlation network centered on N and P, which interconnects K, Mg, Fe, Cu, Zn, and B, while a significant antagonistic relationship between K and Na is also observed.

Correlation analysis of mineral elements in the scion of graft-incompatible 'Dinosaur Egg' combinations (Figure 3B) demonstrated that N exhibited a highly significant positive correlation with K and Na ($p < 0.01$), forming an N-K-Na synergistic network. P showed a highly significant positive correlation with Fe ($p < 0.01$), but highly significant negative correlations with Mg and Mo ($p < 0.01$), establishing antagonistic relationships between P-Fe and Mg-Mo. The positive correlation between K and Na further exacerbated ionic imbalance. Additionally, Ca displayed highly significant positive correlations with Mn and Mo ($p < 0.01$), while exhibiting a highly significant negative correlation with Cu ($p < 0.01$). Mg demonstrated a highly significant positive correlation with Mo ($p < 0.01$) but a highly significant negative correlation with Fe ($p < 0.01$), which in turn showed a highly significant negative correlation with Mo ($p < 0.01$), forming a cross-antagonistic network comprising Ca-Mn-Mo and Mg-Fe. Furthermore, Mn exhibited a highly significant negative correlation with Cu ($p < 0.01$), while Cu displayed highly significant positive correlations with Zn and B ($p < 0.01$). Zn also showed a highly significant positive correlation with B ($p < 0.01$), constituting a Cu-Zn-B synergistic cluster. Collectively, synergistic and antagonistic relationships among elements were intricately intertwined, reflecting dysregulation of the mineral element network in the graft-incompatible scion.

Correlation analysis of mineral elements in graft-incompatible ‘Dinosaur Egg’ rootstocks (Figure 3C) demonstrated that N and P both exhibited highly significant negative correlations with Mo ($p < 0.01$), while showing highly significant positive correlations with Mg, Mn, and Zn ($p < 0.01$). This formed an interactive network where N-P-Mg-Mn-Zn synergistically antagonized Mo. K displayed a highly significant positive correlation with Ca ($p < 0.01$), but highly significant negative correlations with Fe and Na ($p < 0.01$). Concurrently, Ca showed a negative correlation with Fe and a positive correlation with B ($p < 0.05$), constituting a K-Ca-B synergistic chain regulating ionic homeostasis by inhibiting Fe and Na. Furthermore, Mg exhibited highly significant positive correlations with Mn, Cu, and Zn ($p < 0.01$). Fe showed a highly significant positive correlation with Na ($p < 0.01$), while Mn displayed positive correlations with Cu and Zn ($p < 0.01$) but a negative correlation with Mo ($p < 0.01$). Cu was positively correlated with Zn ($p < 0.01$), and Mo with Na ($p < 0.01$). Collectively, synergistic clusters centered on N-P and K-Ca coexisted with localized Mo-Na interactions, revealing disordered synergistic-antagonistic relationships that reflect dysregulation of the mineral element network in graft-incompatible rootstocks.

Correlation analysis between scion and rootstock in graft-incompatible ‘Dinosaur Egg’ combinations (Figure 3D) demonstrated that scion N exhibited highly significant negative correlations with rootstock N, P, Mg, and Mn ($p < 0.01$), but highly significant positive correlations with rootstock Mo and Na ($p < 0.01$), a network is formed in which N-Mo-Na interact synergistically while N-P-Mg-Mn interact antagonistically. Scion P displayed highly significant positive correlations with rootstock N, P, Mg, Mn, Cu, and Zn ($p < 0.01$), this process enhances the synergistic accumulation between P and both macronutrients and micronutrients.

Scion K showed highly significant negative correlations with rootstock N, P, and Mn ($p < 0.01$), but a highly significant positive correlation with rootstock Mo ($p < 0.01$), suggesting K accumulation was inhibited by rootstock N-P-Mn yet promoted by Mo. Scion Ca exhibited a highly significant negative correlation with rootstock Fe ($p < 0.01$) and highly significant positive correlations with rootstock K, Ca, and B ($p < 0.01$), an ionic equilibrium chain was established with synergistic Ca-K-B interactions and antagonistic effects against Fe. Scion Mg demonstrated highly significant negative correlations with rootstock N, P, Mg, Mn, Cu, and Zn ($p < 0.01$), reflecting competitive inhibition between Mg and multiple elements. Simultaneously, scion Fe showed highly significant positive correlations with rootstock N, P, Mg, Mn, Cu, and Zn ($p < 0.01$), while scion Mn exhibited a highly significant negative correlation with rootstock Fe ($p < 0.01$) but highly significant positive correlations with rootstock K, Ca, and B ($p < 0.01$), constituting a redox regulatory network where Fe synergized with multiple elements and Mn antagonized Fe. Scion Cu displayed highly significant negative correlations with rootstock K, Ca, and B ($p < 0.01$) and highly significant positive correlations with rootstock Fe and Na ($p < 0.01$). Both scion Zn and B exhibited highly significant negative correlations with rootstock K ($p < 0.01$) and positive correlations with rootstock Fe, Mo, and Na ($p < 0.01$). Scion Mo showed highly significant negative correlations with rootstock Cu and Zn ($p < 0.01$) but highly significant positive correlations with rootstock Ca and B ($p < 0.01$). Scion Na demonstrated highly significant negative correlations with rootstock N, P, Mg, and Mn ($p < 0.01$) and a highly significant positive correlation with rootstock Mo ($p < 0.01$). Thus, an interconnected and mutually antagonistic network between Cu-Zn-B and Fe-Na-Mo is collectively established. The graft-incompatible scion-rootstock combination exhibits a complex interplay of disordered synergistic and antagonistic relationships among mineral elements, reflecting a systemic dysregulation within the mineral nutrient network between the rootstock and scion under incompatible conditions.

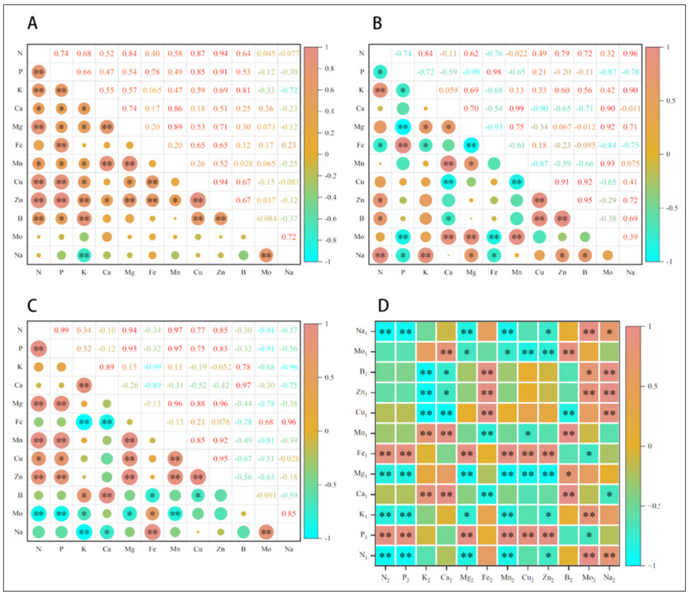

Figure 3: Pearson’s Correlation Coefficients of Mineral Elements in the Graft-Incompatible ‘Dinosaur Egg’ Pluot Combination: Correlation Matrix of 12 Mineral Elements in Graft-Compatible ‘Dinosaur Egg’ Combinations (A); Correlation Matrix of 12 Mineral Elements in Scions of Graft-Compatible ‘Dinosaur Egg’ Combinations (B); Correlation Matrix of 12 Mineral Elements in Rootstocks of Graft-Compatible ‘Dinosaur Egg’ Combinations (C); Correlation Matrix of Mineral Elements Between Scions and Rootstocks in Graft-Compatible ‘Dinosaur Egg’ combinations (D). In (A, B, C, D), Red indicates Positive Correlations and Blue Indicates Negative Correlations, * Represented the Significant Difference at P $p < 0.05$ level, and ** Represented the Significant Difference at $p < 0.01$ level. (D)The Subscript “1” on the Ordinate (Y-axis) Denotes the Scion, while the Subscript “2” on the Abscissa (X-axis) Represents the Rootstock.

Principal Component Analysis of Mineral Elements in 'Dinosaur Egg' pluot Combinations with Varying Graft Compatibility

Principal component analysis (PCA; Figure 4) of 12 mineral elements in graft-compatible and graft-incompatible 'Dinosaur Egg' combinations, including their scions and rootstocks, revealed that the first two principal components (PCs) accounted for 61.1% and 26.1% of variance, respectively, with a cumulative contribution rate of 87.2%, this indicates that these components capture the majority of data variability. Consequently, the two principal components were extracted as comprehensive evaluation indicators for mineral elements in combinations with different graft compatibilities and their respective rootstocks/scions. Loading distribution analysis demonstrated that in PC1, Zn, Ca, Mg, Mn, B, and K exhibited high positive loadings with strong correlations, indicating synergistic interactions. Mo was the only variable with negative loading in PC1, showing the lowest value. However, in PC2, Mo shows the highest loading, followed by N, Fe, and Cu, where Mo, N, and Fe display positive loadings, whereas Cu exhibits a negative loading.

Analysis of sample distributions (Figure 4) indicated that the mineral element profile of compatible 'Dinosaur Egg' grafts was strongly associated with elements including Cu, Mn, B, and Mg. Within compatible combinations, the scion exhibited a mineral profile consistent with that of the compatible graft union, suggesting that the scion is the primary source of mineral elements in these assemblies. In contrast, the rootstock showed a markedly divergent mineral profile compared to both the compatible graft combination and the scion. The mineral characteristics of incompatible 'Dinosaur Egg' grafts were strongly linked to Mo and displayed oppositional patterns along both PC1 and PC2 axes relative to compatible combinations. The rootstock of incompatible grafts closely aligned with the elemental profile of the incompatible combination, indicating that the rootstock constitutes the core source of mineral elements in incompatible assemblies. Meanwhile, the scion of incompatible grafts was strongly associated with N, P, and Fe, and exhibited oppositional characteristics along the PC2 axis compared to the scion of compatible grafts.

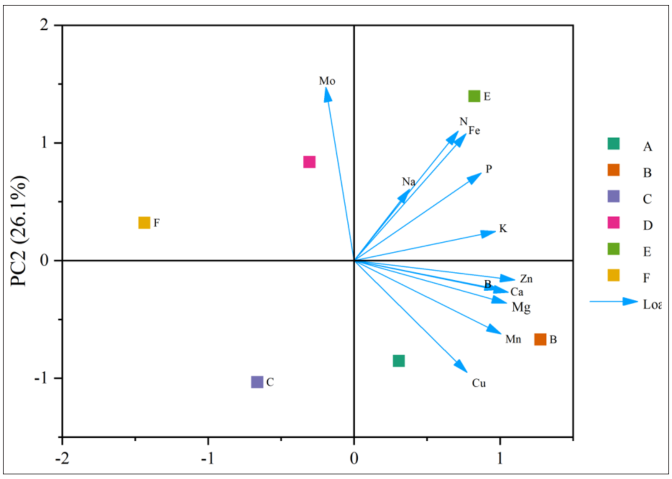

Figure 4: Principal Component Analysis (PCA) of 12 Mineral Elements in Grafted Compatible/Incompatible 'Dinosaur Egg' Combinations and their Rootstocks and Scions, Compatible Grafting Combination (A), Compatible Scion (B), Compatible Rootstock (C); Incompatible grafting Combination (D), Incompatible Scion (E), Incompatible Rootstock (F).

Overall, the graft-compatible 'Dinosaur Egg' combinations, graft-incompatible 'Dinosaur Egg' combinations, as well as their respective rootstocks and scions, showed a significantly opposing distribution along PC1 and PC2. These combinations further formed distinct "compatibility clusters" and "incompatibility clusters" respectively. This result indicates a significant correlation between the overall differentiation of element characteristics and graft compatibility.

Discussion

Mineral nutrient uptake and utilization efficiency constitutes a key factor affecting grafting compatibility in plants [38-40]. Phenotypic variations associated with mineral elements have been documented in wheat, rice, maize, and peach, with applications in breeding novel wheat and maize varieties [41-46]. Concurrently, mineral elements exhibit synergism and competition during absorption and transport processes within plants. In 'Golden Delicious' apple grafted onto different rootstocks, significant positive correlations were identified between Ca and Mg, P and Cu, and K and Ca in leaves [47]. This study employed 'Dinosaur Egg' grafted onto Siberian Apricot rootstocks as experimental material. We performed significance analysis, correlation analysis, and principal component analysis of 12 mineral elements in scions and rootstocks from graft-compatible and graft-incompatible combinations. This investigation aimed to the synergistic relationships between grafting compatibility and scion-rootstock mineral element interactions in apricot-based 'Dinosaur Egg' grafting systems.

Mineral Profiles and Correlation Analysis in Compatible versus Incompatible 'Dinosaur Egg' pluot Combinations

Visual diagnostics in this study revealed that the graft-compatible combinations exhibited significantly more vigorous overall tree growth compared to graft-incompatible combinations. Principal component analysis (PCA) revealed significant differentiation in overall mineral element characteristics between graft-compatible and graft-incompatible 'Dinosaur Egg' combinations. In graft-compatible systems, physiological homeostasis was primarily maintained through synergistic interactions of metal cations (Ca, Mg) and trace elements (Cu, Zn). Conversely, graft-incompatible combinations exhibited dysregulated accumulation of macronutrients (N, P) and specific trace elements (Fe, Mo). In higher plants, Cu and Mo are critically involved in diverse physiological processes including mitochondrial respiration, nitrogen metabolism, sulfur metabolism, stress responses, and enzymatic activities [48]. Correlation analysis revealed highly significant positive correlations among most mineral elements in both graft-compatible and graft-incompatible 'Dinosaur Egg' combinations, forming tightly interconnected synergistic networks. However, in graft-compatible systems, Cu and Mo exhibited highly significant negative correlations, likely due to Cu's involvement in Mo-cofactor biosynthesis, while showing negligible correlations with other elements, forming an antagonistic pair independent of the main network [49]. Conversely, in graft-incompatible combinations, Na and Mo demonstrated negligible correlations with other elements, creating a distinct paradoxical correlation characterized by a local association cluster (Mo-Na) coupled with an antagonistic pair (Na-K). Collectively, while robust synergistic interactions predominated in both systems, the distribution patterns of all 12 mineral elements in graft-incompatible combinations deviated fundamentally from core trends in compatible systems, suggesting scion-rootstock mineral imbalance as the primary determinant of graft incompatibility.

Influence of Scion Mineral Characteristics on Graft Compatibility of 'Dinosaur Egg' pluot

In grafting systems, rootstocks predominantly mediate mineral element absorption essential for plants, with efficiency varying significantly among rootstock genotypes [50]. Studies demonstrate that rootstocks substantially influence mineral composition (including Ca, Cu, K, Mg, Mn, Na, P, S, Zn, and Mo) in apple scions, where specific rootstocks elevate Cu, K, P, and Na levels in scion leaves [47]. However, reported no rootstock-induced alterations in absolute contents of K, Na, Fe, Mn, Cu, or Zn in lemon leaves [51]. In this study, scions from graft-compatible and graft-incompatible 'Dinosaur Egg' combinations showed non-significant differences in four elements: K, Fe, Mo, and Na. This indicates intact ion transport channels for these elements and/or alternative regulatory networks, rendering their concentrations unaffected by grafting compatibility or rootstock variation. These observations are consistent with reports by [52-54].

N and P constitute core elements for plant metabolism and energy synthesis, where abnormal concentrations may directly impair scion physiological function [55]. In this experiment, scions from graft-incompatible 'Dinosaur Egg' combinations exhibited significantly elevated N and P content exclusively compared to graft-compatible counterparts. Principal component analysis (PCA) revealed that graft-compatible scions aligned with overall graft-compatible combination profiles and showed strong correlations with six mineral elements including Ca and Mg [56]. Excessive N and P disrupt rootstock-scion growth equilibrium, causing metabolic hyperactivity and overgrowth in scions [57]. However, limited rootstock transport capacity leads to nutrient partitioning disorders, ultimately manifesting as anatomical compatibility impairments that induce morphological imbalances like the "large and small feet" phenomenon [58]. Conversely, deficiencies in Ca and Mg compromise cellular structural stability and enzymatic activities, adversely affecting chlorophyll synthesis, photosynthesis, and energy metabolism, resulting in leaf chlorosis and growth impairment [59,60].

Correlation analysis revealed that mineral elements in scions from graft-compatible 'Dinosaur Egg' combinations exhibited a homeostatic metabolic pattern characterized by an "N-Mo regulatory axis + K-Ca synergistic cluster," facilitating substance exchange and metabolic coordination between rootstock and scion. Conversely, scions in graft-incompatible combinations exhibit disrupted associations of core elements alongside chaotic distributions of synergistic and antagonistic interactions, which may contribute to dysfunctions at the graft union and imbalances in growth (Xia et al., 2025).

Influence of Rootstock Mineral Characteristics on Graft Compatibility of 'Dinosaur Egg' pluot

Rootstocks of graft-compatible and graft-incompatible 'Dinosaur Egg' combinations showed no significant differences in most mineral elements. However, compatible rootstocks accumulated higher levels of P, K, and trace elements (Cu, Zn), which are essential for energy metabolism, material transport, and enzymatic activities [61,62]. The enrichment of these elements in compatible rootstocks may facilitate energy supply and help maintain physiological homeostasis in scions, consistent with the enhanced tree vigor and growth performance observed in graft-compatible combinations in this study. Studies indicate functional similarities between Na and K enable versatile utilization; while Na cannot fully substitute K, it becomes particularly crucial under K-deficient conditions [63,64]. Principal Component Analysis (PCA) revealed that graft-incompatible rootstocks and graft-incompatible combinations share consistent mineral element characteristics-both exhibit strong association with molybdenum (Mo) and demonstrate a pattern of low potassium (K) and high sodium (Na) levels. This phenomenon may be related to physiological activities such as osmotic regulation, ion homeostasis, and substance exchange between rootstock and scion [65].

Correlation analysis revealed mineral element associations in graft-compatible 'Dinosaur Egg' rootstocks formed a "Cu-antagonistic cluster" with Cu as the negative hub. This cluster comprised nine elements potentially maintaining homeostasis by inhibiting over-accumulation of mutually correlated elements like N and P, while K and Mg remained decoupled from the network, this correlation is consistent with the findings reported [66]. Conversely, graft-incompatible rootstocks exhibited fragmented correlations characterized by multiple antagonistic pairs and localized synergies without a unifying core, potentially disrupting Cu-cluster homeostasis. These results indicate critical importance of rootstock-to-scion nutrient transport efficiency. The K-depleted/Na-enriched status and insufficient P, Cu, Zn uptake in incompatible rootstocks cause scion nutrient deprivation, thereby inducing compatibility barriers (ZHANG et al., 2010, but precise mechanisms require further elucidation [67].

Mineral Element Distribution and Correlation Between Scion and Rootstock Influence Graft Compatibility in 'Dinosaur Egg' Pluot

Scions in both graft-compatible and graft-incompatible 'Dinosaur Egg' combinations showed higher concentrations of seven mineral elements (including N and P) than their corresponding rootstocks, indicating minimal correlation between these distribution patterns and grafting compatibility on Siberian Apricot rootstocks. Although rootstocks exhibited non-significant differences in most mineral elements between compatibility groups, their scions however displayed significant variations in eight elements. Most elements were elevated in scions from compatible combinations compared to incompatible counterparts. Consequently, differential nutrient supply in scions may contribute to graft incompatibility [68]. In Arabidopsis, excess Fe and Cu significantly altered CalSs and PDBG concentrations, ultimately impairing intercellular signaling efficiency [69,70]. In graft-incompatible 'Dinosaur Egg' combinations, K, Fe, and Cu transport efficiencies between rootstock and scion were significantly lower than in compatible combinations, causing abnormal elemental accumulation in scions that may trigger ionic toxicity or metabolic disorders [71-74]. It is hypothesized that resultant transport channel dysfunction or regulatory mechanism imbalance constitutes a primary factor in reduced grafting compatibility. Impaired transport of K, Fe, and Cu in graft-incompatible systems may associate with abnormal expression/activity of channel proteins (transporters, channel enzymes) at rootstock-scion junctions, requiring molecular validation. Non-significant Mo content differences between graft-compatible and -incompatible 'Dinosaur Egg' rootstocks/scions indicate minimal linkage between Mo uptake/transport and grafting compatibility, suggesting the presence of physiological mechanisms mediated by networks that operate independently of the grafting system [75]. Similarly, Na content showed non-significant differences both within rootstock/scion pairs of incompatible combinations and between scions across compatibility groups, implying Na transport likely occurs via exclusive ion channels unaffected by rootstock type or compatibility status [76].

Principal component analysis (PCA) of spatial distribution and correlations revealed that graft-compatible 'Dinosaur Egg' combinations formed tightly clustered affinity groups with Cu as the negative correlation hub in scion-rootstock associations, establishing an N-P-K-Cu metabolic-transport regulatory chain that maintains synergistic multi-element supply in scions [77, 78]. Conversely, graft-incompatible combinations exhibited incompatibility groups dominated by antagonistic mineral element interactions, the P-Fe-Mo-Na toxicity-osmosis conflict chain induced localized dysregulation, potentially causing network fragmentation, impaired nutrient transport at graft unions, and imbalanced rootstock/scion mineral allocation [79,80]. Thus, mineral-element associations in graft-compatible 'Dinosaur Egg' combinations exhibited network configurations centered on key elements, with clearly clustered positive/negative correlations. Conversely, graft-incompatible combinations displayed fragmented associations characterized by disjointed "micro-clusters + multi-antagonism" patterns in rootstock-scion systems.

Overall, in compatible 'Dinosaur Egg' graft combinations, Cu functioned as the core negative regulator establishing a multi-element synergistic network that maintained nutrient homeostasis. The orderly interactions between elements enabled Cu to serve as a potential "biochemical marker" for graft affinity, providing guidance for nutrient regulation. Conversely, in incompatible 'Dinosaur Egg' graft combinations, elemental imbalance resulted from "multi-group antagonism coupled with localized synergism", which compromised nutrient supply to scions and disrupted elemental associations. Future research should focus on mineral element balance regulation by employing bioinformatics approaches to validate how channel protein expression affects mineral element transport between rootstocks and scions, while exploring targeted element application methods to improve grafting affinity [81,82]. Utilizing gene editing techniques such as CRISPR/Cas9 or RNA silencing to screen rootstock varieties with high transport efficiency for K, Fe, and Cu could reduce scion element accumulation risks and enhance graft compatibility [83-85]. Concurrently, Mo and Na may serve as "non-sensitive markers" or "stabilizing reference elements" in grafting experiments to eliminate transport interference and calibrate experimental data, their transport independence could provide control benchmarks for such studies [86].

Conclusion

Grafting compatibility of 'Dinosaur Egg' (Prunus domestica × P. armeniaca 'Konglongdan') pluot on Siberian Apricot (Armeniaca sibirica (L.) Lam.) rootstocks is regulated by synergistic mineral element effects in the rootstock-scion system. Enrichment of P, K, Cu, and Zn in rootstocks optimizes scion nutrition. However, excessive accumulation of N, P, K, Fe, and Cu in scions reduces compatibility. Concurrently, localized Mo-Na associations and K-Na imbalance (low K/high Na) in rootstocks further diminish compatibility. Compatibility is enhanced when elements exhibit ordered synergism and antagonism, whereas the absence of a unified regulatory hub causing disorganized elemental interactions reduces compatibility. Overall, coordinated interactions among Ca, Mg, Mn, Cu, Zn, and B promote compatibility in these graft combinations, while aberrant associations involving P, Fe, and Na decrease it. Crucially, Cu functions as the core regulatory hub for compatibility, with excess N and P combined with deficiencies in Ca, Mg, K, Zn, Mn, and B constituting primary drivers of incompatibility. Mo, Fe, and Na indirectly modulate compatibility through elemental balance regulation, where maintaining "integrity of the elemental synergistic network" and "equilibrium of core element content" is fundamental [87-91].

Acknowledgement: The author(s) declare financial support was received for the research, authorship, and/or publication of this article. This work was funded by the Key Research and Development Project of the Autonomous Region: "Research and Demonstration on Elite Cultivar Selection and Propagation Techniques for Xinjiang Prunes and Pluot"(2023B02016-3) and Innovative Research Group Project of the Autonomous Region University Scientific Research Program: "Evaluation of Xinjiang Apricot Germplasm Resources and Breeding of New Varieties"(XJEDU2007T05).

Author Contributions: M.L. and Y.H. Conceptualization, Methodology, Investigation, Data curation and Formal analysis, Visualization and Writing–original draft; T.G. : Project administration, Supervision, Writing–review & editing; M.W. : Funding acquisition, Supervision, Writing–review & editing; X.W.: Conceptualization, Methodology, Funding acquisition, Writing–review & editing. All authors have read and agreed to the published version of the manuscript.

Data Availability Statement: The original contributions presented in this paper are included in this article; further inquiries can be directed to the corresponding author.

Conflict of Interest: The authors declare that the research was conducted in the absence of any commercial or financial relationships that could be construed as a potential conflict of interest.

References

1. Yaxin L, Jiajia Z, Shaobin Y, Jun T, Yingying W (2022) Flowering biological characteristics of 6 prunusdomestica× armeniaca varieties. J Northwest A F Univ Nat Sci Ed 50: 84-90.
2. Wei Y, Liao K, Li W, Feng B, Xu Y, et al. (2017) An anatomical study on flower bud differentiation in prunus salicina× armeniaca. J Fruit Sci 34: 840-850.
3. Fang DL, Hong YD, Dali F, Shao BY (2004) 'Konglongdan'-a new cultivar of hybrid between the species of plum and apricot. Acta Hortic Sin 835.
4. Du Gai, Li Taishan, Diao Songfeng, Zhang Jiajia, Fu J, et al. (2017) Evaluation of flavor quality in relation to sugars and acids of six prunus domestica× armeniaca cultivars. J Fruit Sci 34: 41-49.
5. Jinqiu W, Haikun B, Chu W, Mingyu Y, Mengzhen H, et al. (2025) Effects of different rootstock-scion combinations on fruit size and quality of apricot. J Northwest A F Univ Nat Sci Ed: 1-11. https://doi.org/10.13207/j.cnki.jnwafu.2025.09.010.
6. Yaozhan Z, Yanhong Y, Suling W, Xiangyang C (2004) Mid-early ripening pluot varieties and their cultivation techniques. North Hortic 5: 34-35.
7. Ruyue W, Haifang H, Shasha L, Ziyi Z, Yeyong X (2025) Fruit quality analysis of prunus domestica × armeniaca at different harvest maturity levels. J Agric Sci Technol 27: 158-169.
8. Wei J, Li Y, Liang Y (2023) Advances in research on improving tomato disease resistance and stress resistance by grafting technology. Acta Hortic Sin 50: 1997-2014.
9. He W, Xie R, Wang Y, Chen Q, Wang H (2022) Comparative transcriptomic analysis on compatible/incompatible grafts in citrus. Hortic Res 9: uhab72.
10. Wang L, Liao Y, Liu J, Zhao T, Jia L (2024) Advances in understanding the graft healing mechanism: a review of factors and regulatory pathways. Hortic Res 11: 1-13.
11. Ganiyu SA, Popoola AR, Nekomimi OA, Bodunde JG (2020) Evaluation of integrated management of bacterial wilt of tomato using grafting, biofumigant and plant resistance activator under field conditions. Austral Plant Pathol 49:

249-255.
12. Kirca L, Karadeniz T (2024) Histological investigation of the compatibility of prunus spinosa as interstock with almond cultivars. Appl Fruit Sci 66: 1305-1316.
13. Lordan J, Zazurca L, Maldonado M, Torguet L, Alegre S (2019) Horticultural performance of 'marinada' and 'vairo' almond cultivars grown on a genetically diverse set of rootstocks. Sci Hortic 256: 108558.
14. Loupit G, Brocard L, Ollat N, Cookson SJ (2023) Grafting in plants: recent discoveries and new applications. J Exp Bot 74: 2433-2447.
15. Habibi F, Liu T, Folta K, Sarkhosh A (2022) Physiological, biochemical, and molecular aspects of grafting in fruit trees. Hortic Res 9: uhac32.
16. Tripathi R, Tewari R, Singh KP, Keswani C, Minkina T (2022) Plant mineral nutrition and disease resistance: a significant linkage for sustainable crop protection. Front Plant Sci 13: 883970.
17. Reed JF (2019) Visual plant symptoms as indicators of mineral nutrient deficiencies. Detecting Mineral Nutrient Deficiencies in Tropical and Temperate Crops: 1-12. https://doi.org/10.1201/9780429035258-1.
18. Kuzin A, Solovchenko A (2021) Essential role of potassium in apple and its implications for management of orchard fertilization. Plants 10: 2624.
19. Liu Y, Ding W, He P, Xu X, Zhou W (2024) Estimating thresholds of nitrogen, phosphorus and potassium fertilizer rates for rice cropping systems in china. Front Plant Sci 15: 1470774.
20. Cruz AF, Almeida GMD, Wadt PGS, Pires MDC, Ramos MLG (2019) Seasonal variation of plant mineral nutrition in fruit trees. Braz Arch Biol Technol 62: e19180340.
21. De Bang TC, Husted S, Laursen KH, Persson DP, Schjoerring JK (2021) The molecular-physiological functions of mineral macronutrients and their consequences for deficiency symptoms in plants. New Phytol 229: 2446-2469.
22. Lilay GH, Thiébaut N, du Mee D, Assunção AG, Schjoerring JK (2024) Linking the key physiological functions of essential micronutrients to their deficiency symptoms in plants. New Phytol 242: 881-902.
23. Chunxiang L, Yongbo H, Guojie Q, Li C (2021) Technology and application of fruit seedling raising of prunus tomentosa. North Hortic: 174-176. https://doi.org/10.11937/bfyy.20205525.
24. Mingyan L, Yue P, Lu A, Dongya Z, Fuwei Z (2018) Comprehensive evaluation of salt tolerance of prunus domestica × armeniaca stock based on principal component analysis. Jiangsu Agric Sci 46: 105-109.
25. Jianmin F, Shuzhan L, Lanying D (2008) Grafting techniques of hybrid between the species of plum and apricot on a new cultival "fengweimeigui". North Hortic: 31-32.
26. Shang-Kun W, Chuan-lai Z (2012) Research progress of plumcot. North Hortic 194-200.
27. Lynch JP (2007) Roots of the second green revolution. Aust J Bot 55: 493-512.
28. Hodge A, Berta G, Doussan C, Merchan F, Crespi M (2009) Plant root growth, architecture and function. Plant Soil 321: 153-187.
29. Kuijken RC, van Eeuwijk FA, Marcelis LF, Bouwmeester HJ (2015) Root phenotyping: from component trait in the lab to breeding. J Exp Bot 66: 5389-5401.
30. Reig G, Zarrouk O, Font I Forcada C, Moreno MÁ (2018) Anatomical graft compatibility study between apricot cultivars and different plum based rootstocks. Sci Hortic 237: 67-73.
31. Reig G, Salazar A, Zarrouk O, Forcada CFI (2019) Long-term graft compatibility study of peach-almond hybrid and plum based rootstocks budded with european and Japanese plums. Sci Hortic 243: 392-400.
32. Moreno MA, Moing A, Lansac M, Gaudillère JP, Salesses G (1993) Peach/myrobalan plum graft incompatibility in the nursery. J Hortic Sci 68: 705-714.
33. Scholten HJ, Hartman HT, Kester DE, Davies FT, Geneve RL (1963) Plant propagation: principles and practices. Soil Sci 95.
34. Amri R, Font I Forcada C, Giménez R, Pina A, Moreno MÁ (2021) Biochemical characterization and differential expression of pal genes associated with "translocated" peach/plum graft-incompatibility. Front Plant Sci 12: 622578.
35. Juan D, Yan-Hua W, Jing S, Run-Rong YE, Xue-feng LU (2015) Determination of 21 mineral elements in two species of comastoma by icp-oes. Nat Prod Res Dev 27: 837-841.
36. Chen S, Mu D, Wang Y, Chen L, Tang J (2023) Study on the excellence of smartchem 200 automatic chemical analyzer in rapid determination of nitrogen and phosphorus of seedlings. J West China for Sci 52: 77-82.
37. Rui M, Yong L, Weijun W (2025) Determination of 15 elements in black tea by inductively coupled plasma mass spectrometry. Chin J Inorg Anal Chem 15: 1228-1237.
38. Huang Y, Zhao L, Kong Q, Cheng F, Niu M (2016) Comprehensive mineral nutrition analysis of watermelon grafted onto two different rootstocks. Hortic Plant J 2: 105-113.
39. Nawaz MA, Imtiaz M, Kong Q, Cheng F, Ahmed W (2016) Grafting: a technique to modify ion accumulation in horticultural crops. Front Plant Sci 7: 1-15.
40. Warschefsky EJ, Klein LL, Frank MH, Chitwood DH, Londo JP (2016) Rootstocks: diversity, domestication, and impacts on shoot phenotypes. Trends Plant Sci 21: 418-437.
41. Valle SR, Pinochet D, Calderini DF (2011) Uptake and use efficiency of n, p, k, ca and al by al-sensitive and al-tolerant cultivars of wheat under a wide range of soil al concentrations – science direct. Field Crops Res 121: 392-400.
42. Hakeem KR, Chandna R, Ahmad A, Iqbal M (2012) Physiological and molecular analysis of applied nitrogen in rice genotypes. Rice Sci 19: 213-222.
43. Mundim GB, Viana JMS, Maia C, Paes GP, DeLima RO (2013) Genetic diversity and path analysis for nitrogen use efficiency in popcorn inbred lines. Euphytica 191: 291-299.
44. Reighard GL, Bridges W, Rauh B, Mayer NA (2012) Prunus rootstocks influence peach leaf and fruit nutrient content. In: VII International Symposium on Mineral Nutrition of Fruit Crops (ed.).
45. Daneshbakhsh B, Khoshgoftarmanesh AH, Shariatmadari H, Cakmak I (2013) Phytosiderophore release by wheat genotypes differing in zinc deficiency tolerance grown with zn-free nutrient solution as affected by salinity. J Plant Physiol 170: 41-46.
46. Zhang Y, Chen F, Chen X, Long L, Kun G (2013) Genetic improvement of root growth contributes to efficient phosphorus acquisition in maize (zea mays l.). J Integr Agric 12: 1098-1111.
47. Fazio G, Kviklys D, Grusak MA, Robinson T (2013) Phenotypic diversity and qtl mapping of absorption and translocation of nutrients by apple rootstocks. Asp Appl Biol 119: 37-50.
48. Hänsch R, Mendel RR (2009) Physiological functions of mineral micronutrients (cu, zn, mn, fe, ni, mo, b, cl). Curr Opin Plant Biol 12: 259-266.
49. Kuper J, Llamas A, Hecht H, Mendel RR, Schwarz G (2004) Structure of the molybdopterin-bound cnx1g domain links molybdenum and copper metabolism. Nature 430: 803-806.

50. Koepke T, Dhingra A (2013) Rootstock scion somatogenetic interactions in perennial composite plants. Plant Cell Rep 32: 1321-1337.
51. Almansa MS, Hernandez JA, Jimenez A, Botella MA, Sevilla F (2002) Effect of salt stress on the superoxide dismutase activity in leaves of citrus limonum in different rootstock-scion combinations. Biol Plant 45: 545-549.
52. Tsipouridis C, Thomidis T (2005) Effect of 14 peach rootstocks on the yield, fruit quality, mortality, girth expansion and resistance to frost damages of may crest peach variety and their susceptibility on phytophthora citrophthora. Sci Hortic 103: 421-428.
53. Cabrera RI (2002) Rose yield, dry matter partitioning and nutrient status responses to rootstock selection. Sci Hortic 95: 75-83.
54. Sherafati A, Hokmabadi H, Taheri M (2011) Effects of some rootstocks on mineral nutrient uptake in two pistachio cultivars (pistacia vera l.). Acta Hortic 912: 197-201.
55. Nunes-Nesi A, Fernie AR, Stitt M (2010) Metabolic and signaling aspects underpinning the regulation of plant carbon nitrogen interactions. Mol Plant 3: 973-996.
56. Hrotkó K, Magyar L, Borsos G, Gyeviki M (2014) Rootstock effect on nutrient concentration of sweet cherry leaves. J Plant Nutr 37: 1395-1409.
57. Yujie T, Xiaorui L, Junping L, Zhuangzhuang L, Fangren P (2022) Effects of different rootstocks on growth and mineral elements in leaf of grafted pecan seedlings. J Southwest for Univ 42: 18-25.
58. Rasool A, Mansoor S, Bhat KM, Hassan GI, Baba TR (2020) Mechanisms underlying graft union formation and rootstock scion interaction in horticultural plants. Front Plant Sci 11: 590847.
59. McMurtrey JE (1938) Distinctive plant symptoms caused by deficiency of any one of the chemical elements essential for normal development. Bot Rev 4: 183-203.
60. Suman M, Sangma PD, Singh D (2017) Role of micronutrients (fe, zn, b, cu, mg, mn and mo) in fruit crops. Int J Curr Microbiol Appl Sci 6: 3240-3250.
61. Krmer U, Clemens S (2005) Functions and homeostasis of zinc, copper, and nickel in plants. Springer Berlin Heidelberg: 215-271. https://doi.org/10.1007/4735_96.
62. Sardans J, Peñuelas J (2021) Potassium control of plant functions: ecological and agricultural implications. Plants 10: 419.
63. Maathuis FJ (2014) Sodium in plants: perception, signalling, and regulation of sodium fluxes. J Exp Bot 65: 849-858.
64. Raddatz N, Morales De Los Ríos L, Lindahl M, Quintero FJ, Pardo JM (2020) Coordinated transport of nitrate, potassium, and sodium. Front Plant Sci 11: 247.
65. Wakeel A, Farooq M, Qadir M, Schubert S (2011) Potassium substitution by sodium in plants. Crit Rev Plant Sci 30: 401-413.
66. Ibacache G A, Sierra B C (2009) Influencia de portainjertos sobre el contenido peciolar de nitrógeno, fósforo y potasio en cuatro variedades de uva de mesa. Chil J Agric Res 69: 503-508.
67. Chang C, Chao LI, Li C, Kang X, Zou Y (2014) Differences in the efficiency of potassium (k) uptake and use in five apple rootstock genotypes. J Integr Agric 13: 1934-1942.
68. Hollick JR, Kubota C (2022) Effect of self-and inter-cultivar grafting on growth and nutrient content in sweet basil (ocimum basilicum l.). Front Plant Sci 13: 921440.
69. Müller J, Toev T, Heisters M, Teller J, Moore KL (2015) Iron-dependent callose deposition adjusts root meristem maintenance to phosphate availability. Dev Cell 33: 216-230.
70. Lexy R, Kasai K, Clark N, Fujiwara T, Sozzani R (2018) Exposure to heavy metal stress triggers changes in plasmodesmatal permeability via deposition and breakdown of callose. J Exp Bot 69: 3715-3728.
71. Dogra K, Kour K, Kumar R, Bakshi P, Kumar V (2018) Graft-incompatibility in horticultural crops. Int J Curr Microbiol Appl Sci 7: 1805-1820.
72. Nagajyoti PC, Lee KD, Sreekanth TVM (2010) Heavy metals, occurrence and toxicity for plants: a review. Environ Chem Lett 8: 199-216.
73. Küpper H, Andresen E (2016) Mechanisms of metal toxicity in plants. Metallomics 8: 269-285.
74. Zahra N, Hafeez MB, Shaukat K, Wahid A, Hasanuzzaman M (2021) Fe toxicity in plants: impacts and remediation. Physiol Plant 173: 201-222.
75. Martínez-Ballesta MC, Alcaraz-López C, Muries B, Mota-Cadenas C, Carvajal M (2010) Physiological aspects of rootstock--scion interactions. Sci Hortic 127: 112-118.
76. Schmutz U, Lüdders P (1999) Effect of nacl salinity on growth, leaf gas exchange, and mineral composition of grafted mango rootstocks (var.'13-1'and 'turpentine'). Gartenbauwissenschaft 64: 60-64.
77. Albacete A, Martínez-Andújar C, Martínez-Pérez A, Thompson AJ (2015) Unravelling rootstock× scion interactions to improve food security. J Exp Bot 66: 2211-2226.
78. Rasool A, Mansoor S, Bhat KM, Hassan GI, Baba TR (2020b) Mechanisms underlying graft union formation and rootstock scion interaction in horticultural plants. Front Plant Sci 11: 590847.
79. Baron D, Esteves Amaro AC, Pina A, Ferreira G (2019) An overview of grafting re-establishment in woody fruit species. Sci Hortic 243: 84-91.
80. Gautier AT, Chambaud C, Brocard L, Ollat N, Gambetta GA (2019) Merging genotypes: graft union formation and scion–rootstock interactions. J Exp Bot 70: 747-755.
81. Liu Q, Wang X, Zhao Y, Xiao F, Yang Y (2023) Transcriptome and physiological analyses reveal new insights into delayed incompatibility formed by interspecific grafting. Sci Rep 13: 4574.
82. Niu L, Hu W, Wang F, Shaker M, Yang X (2025) Integrated transcriptomic and metabolomic analyses elucidate the mechanism by which grafting impacts potassium utilization efficiency in tobacco. BMC Plant Biol 25: 94.
83. Chilukamarri L, Ashrafzadeh S, Leung DW (2021) In-vitro grafting-current applications and future prospects. Sci Hortic 280: 109899.
84. Jiang L, Shen W, Liu C, Tahir MM (2022) Engineering drought-tolerant apple by knocking down six gh3 genes and potential application of transgenic apple as a rootstock. Hortic Res 9: uhac122.
85. Yang L, Machin F, Wang S, Saplaoura E, Kragler F (2023) Heritable transgene-free genome editing in plants by grafting of wild-type shoots to transgenic donor rootstocks. Nat Biotechnol 41: 958-967.
86. Vanhaecke F, Costas Rodríguez M (2021) High-precision isotopic analysis of essential mineral elements: capabilities as a diagnostic/prognostic tool. View-China 2: 20200094.
87. Luo T, Zhao L, Hu XS (2008) Study on characteristic analysis of mineral elements in green tea and discrimination based on origin. Food Sci 29: 494-497.
88. Taishan L, Wei JH, Gaigai D, Songfeng D, Yanzhi F (2017) Volatile characteristics of different prunus domestica× armeniaca cultivars evaluated by hs-spme with gc-ms. Sci Silvae Sin 53: 123-132.

89. Xia C, Miranda J, Mendoza Cozatl D (2025) Decoding long-distance communication under mineral stress: advances in vascular signalling and molecular tools for plant resilience. Plant Cell Environ 48: 4781-4802.
90. Yang L, Xia L, Zeng Y, Han Q, Zhang S (2022) Grafting enhances plants drought resistance: current understanding, mechanisms, and future perspectives. Front Plant Sci 13: 1015317.
91. Zikun Z, Hua LI, Yu Z, Zhijun H, Kun C (2010) Grafting enhances copper tolerance of cucumber through regulating nutrient uptake and antioxidative system. Agric Sci China 9: 1758-1770.

Copyright: ©2026 Xinjian Wang, et al. This is an open-access article distributed under the terms of the Creative Commons Attribution License, which permits unrestricted use, distribution, and reproduction in any medium, provided the original author and source are credited.